A flexible methanol-to-methane thermochemical energy storage system (TCES) for gas turbine (GT) power production

D.A. Rodriguez-Pastor [a,*], A. Garcia-Guzman [a], I. Marqués-Valderrama [a], C. Ortiz [b], E. Carvajal [a], J.A. Becerra [a,d], V.M. Soltero [c], R. Chacartegui [a,d]

[a] *University of Seville, Escuela Técnica Superior de Ingenieros, Camino de los Descubrimientos s/n, 41092 Seville, Spain*
[b] *University Loyola Andalucía, Av. de Las Universidades s/n, Dos Hermanas, 41704 Seville, Spain*
[c] *University of Seville, Escuela Politécnica Superior, 41011 Seville, Spain*
[d] *University of Seville, Laboratory of Engineering for Energy and Environmental Sustainability, Seville 41092, Spain*

HIGHLIGHTS

- A novel flexible storage system for conventional power generation is proposed.
- Green methanol to methane conversion process from intermediate step to synthesis gas.
- Overall system efficiencies above 29% and roundtrip efficiencies of 44% were achieved.
- Competitive levelized fuel cost of €172/MWh and future LCOE values <€265/MWh are reached.

ARTICLE INFO

ABSTRACT

This study introduces an innovative solution to address the challenges arising from the volatile natural gas market and the growing integration of renewable energy sources within the industrial sector. The research strives to confront this challenge by including renewable methanol (CH_3OH) and converting it into methane (CH_4), with an intermediate step involving synthesis gas (CO/H_2) by using concentrating solar power. This approach provides a sustainable and adaptable solution to reduce dependence on natural gas. The process entails a methanol decomposition reaction at moderate temperatures (<350 °C). Subsequently, the synthesis gas is compressed to 40 bar, stored, and discharged through a methanation process that can be conducted at high temperatures (>500 °C). The resulting methane is used as fuel for gas turbines and can also serve as feedstock in the chemical industry. The simulations were conducted in ASPEN HYSYS and yielded overall system efficiencies exceeding 29% and roundtrip efficiencies of 44%. Through techno-economic optimisation of the reaction conditions, competitive levelized fuel costs (LCOF) of €172/MWh and future LCOE values of €145/MWh were achieved. These findings present an innovative strategy for integrating gas turbine cycles and additional conversion pathways for green methanol.

1. Introduction

The high level of variable renewable energy in the electric grid presents a critical challenge for boosting worldwide energy storage capacity [1,2]. Thermochemical storage (TCES) is a solution for long-term storage in solar power plants, allowing charging (chemical decomposition) and discharging (chemical synthesis) for both daily and seasonal storage approaches [3]. Several reaction pairs are promising for thermochemical energy storage because of their higher energy densities than current sensible and latent energy storage. Some are based on liquid-gas (Isopropanol/acetone (>200 °C) [4]), solid-gas (CaO/CaCO$_3$ [5], CaO/Ca(OH)$_2$ [6], MgO/Mg(OH)$_2$ [7], (>600 °C)) and gas-gas (ammonia (>400 °C) [8], SO$_3$ (800–1000 °C) [9], CH$_3$OH (>300 °C) [10]), among others. Most high-efficiency TCES systems require high temperatures for the decomposition step, which is difficult to achieve with current solar concentrators and increases installation costs [11]. Thus, there is a need for energy carriers that can be produced and stored efficiently and sustainably using renewable sources at intermediate temperatures

---

($<$400 °C).

Methanol (CH_3OH) is a promising alternative energy carrier [12], as it can be produced from renewable sources such as biomass gasification or hydrogenation of industrial effluents [13,14]. It has several advantages over other energy carriers, such as being a liquid fuel under ambient conditions, allowing less expensive transport and storage, and having a higher energy density than hydrogen [15]. Because of its high hydrogen content, it is considered a practical solution for hydrogen transport [16]. Despite some drawbacks, such as toxicity [17], it is a widely used and mature technology with large-scale production in the chemical industry [18]. Methanol is used as a compound for different chemical processes, and there is a relevant activity in adapting power generation systems to this fuel [19–22].

Several studies have investigated methanol production from renewable sources and its conversion to hydrogen or liquid hydrocarbons via different processes, such as reforming, methanation, dimethyl ether synthesis, and Fischer–Tropsch synthesis. Moioli et al. [23] assessed the catalytic conversion of CO_2 and H_2 to methane and methanol. They found that the maximal storage efficiency (total energy stored between total energy spent) was 85.3% for methanol and 78.2% for methane. Garcia et al. [24] reviewed methanol's main hydrogen production processes and reported that the highest hydrogen yield was 3.5 mol H_2/mol CH_3OH, achieved by autothermal reforming. The highest methane production rate by electrochemical methanation from renewable sources, 0.8 mol CH_4/mol CO_2, was obtained by Biswas et al. [25]. Haynes et al. [26] reconsidered the logic of biological methane activation and its conversion to liquid fuels. [26] They suggested paths to produce liquid transportation fuels from methane at high carbon yield, high energy efficiency, and low CO_2 emissions. A review of the conversion of H_2 and CO_2 to liquid fuels via power-to-liquid processes was performed in [27], comparing the techno-economic and environmental performance of different pathways, such as methanol synthesis, dimethyl ether synthesis, and Fischer–Tropsch synthesis. However, no studies have focused on converting methanol to methane as an intermediate step for power generation, where methanol is only decomposed into syngas and then used [28–32]. Moreover, most of these studies have used conventional steam reforming or partial oxidation of methanol, which requires high temperatures and pressures, resulting in CO_2 emissions.

Synthetic (green) natural gas (SNG) is a key energy carrier. Power and heat technologies widely use natural gas in gas turbines, cogeneration engines [33] or chemical industries, gas boilers, and methane reforming processes [34]. Natural gas use is not only limited by reserves and regional accessibility; as recently demonstrated, global conditions significantly influence costs. Traditional SNG production methods typically rely on nonrenewable sources, such as coal. However, there are sustainable approaches that use biomass, landfills, livestock residues, or waste treatment [35]. The production of synthetic natural gas (SNG) from dry lignocellulosic biomass using thermochemical methods is a relatively new concept that has not yet been extensively implemented at an industrial level. It is an early-stage technology with a limited number of small-scale tests and pilot plants in operation [36,37]. The term "Power-to-Gas" refers to converting electrical energy into hydrogen and methane, the latter being synthetic natural gas. Other forms of converting electrical energy into liquid energy carriers ("Power-to-Fuels"), such as hydrocarbons (methanol, dimethyl ether, and Fischer-Tropsch products), can also be used as intermediates for SNG production. The methanation process offers several advantages for SNG production. The resulting product heating value was within the natural gas range. It eliminates the need to accommodate equipment at higher hydrogen concentrations [38].

Moreover, compared with pure hydrogen, SNG, with a methane content ranging from 87% to 97%, has fewer obstacles to implementation. It is safer, easier to transport and store, and better suited for industrial applications [39]. However, SNG production from renewable sources requires multiple steps and high temperatures, which reduce the

efficiency and increase the cost of the process. In addition, injecting SNG into the network or storing it requires high pressure, which penalises the roundtrip efficiency of the process. Finally, when considering methane as an energy storage system (energy vector), it is important to note that the energy density is lower than that of the liquid vectors.

The conversion of renewable methanol to methane or synthetic natural gas (SNG) is an attractive option for storing and transporting renewable energy in liquid fuels and for use in conventional power systems with soft retrofitting. The large-scale production of methanol, storing it (with high energy density, 0.0364 MJ/L CH_4 $<$ 15.6 MJ/L CH_3OH [40]), and the potential conversion of a portion of the produced methanol into methane for industrial use is a novel pathway that has barely been studied in the literature.

This work proposes a novel approach for gas turbine power production based on the conversion of methanol to methane via the innovative integration of known reactions, such as methanol decomposition and methanation, coupled to provide a thermochemical storage and synthetic natural gas (SNG) generation system that can power a commercial gas turbine. Methanol can be produced from renewable sources at moderate temperatures with higher efficiency than synthetic natural gas (SNG). Methanol can also be used as a hydrogen carrier for fuel cells or as feedstock for the chemical industry [41]. However, methanol has a higher volatility and lower density than other fuels, which limits its direct use in some applications. Therefore, converting methanol to methane ($CH4$), which has a higher heating value and can be easily stored and transported using the existing natural gas infrastructure, could be a promising energy storage and utilisation option.

Concretely, this work proposes a novel concept for converting methanol to methane using solar concentrated solar power (CSP) technology, which allows the decomposition of methanol into syngas at moderate temperatures and pressures and the subsequent methanation of syngas into CH_4 without CO_2 emissions. The proposed system can be used as a thermochemical energy storage (TCES) system that can store excess renewable energy in methanol and release it as heat and electricity when needed. The system can operate in two modes: open-loop and closed-loop modes. In the open-loop mode, methanol is constantly fed into the system and converted to heat, electricity, and CH_4 at different stages. This approach is proposed in the patent by Chacartegui et al. [42]. In closed-loop mode, methanol is decomposed into syngas during the charging phase (when renewable energy is available) and stored in tanks. Syngas is then converted to CH_4 during the discharging phase (when renewable energy is unavailable) and used to power a gas turbine.

The resulting synthetic natural gas is around €172/MWh from methanol obtained by biomass gasification with levelized gas turbine power costs below €260/MWh. Relatively high roundtrip efficiencies ($>$40%) have been achieved through techno-economic optimisation and joint integration with solar photovoltaics, ensuring a carbon-neutral system. A synthetic natural gas with a high molar percentage of methane at the outlet ($>$90%) provides a high operational flexibility. It allows using the existing methane transport infrastructure network or direct use in natural gas turbines, acting at peak demand periods, and optimising economic profitability. It is estimated that the biomethanol costs could reach €227/t for higher levels of technology maturity, implying LCOE values around €142/MWh. Similarly, in 2050, the prices of methanol from CO_2 and H_2 with electrolysis could reach €250/t, and the LCOE of the proposed technology would be around €152/MWh, offering a competitive and flexible configuration that would lower the costs of CSP.

2. System description

The methanol-decomposition reaction (Eq. (1)) produces syngas with a 2:1 ratio of hydrogen (H_2) and carbon monoxide (CO) at equilibrium. It has different industrial applications, and the separation of CO from H_2 in a controlled environment allows the latter to serve as fuel

[43]. Current catalysts for methanol decomposition are based on Cu, Pt, Pd, and Ni [44], although Cu-based catalysts are vulnerable to rapid deactivation due to carbon poisoning [45].

$$CH_3OH \leftrightarrow CO + 2H_2 \quad \Delta H_{298 \, K} = 90.7 \, kJ/mol \tag{1}$$
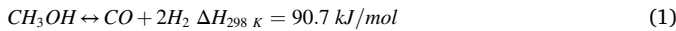
CO methanation (Eq. (2)) is an exothermic reaction that preferentially occurs at low temperatures, according to the LeChatelier principle [46]. However, from a kinetic point of view, high temperatures lead to a faster reaction rate, which is commonly used in the industry to ensure economic profitability, such as in the first-stage methanation reactor in the TREMP™ process with a temperature range of 600–700 °C [47]. Conventional Al_2O_3-supported Ni-based catalysts are most used for CO methanation because they have high catalytic activity, are easy to prepare, and are relatively inexpensive [48].

$$CO + 3H_2 \leftrightarrow CH_4 + H_2O \quad \Delta H_{298 \, K} = -206.1 \, kJ/mol \tag{2}$$
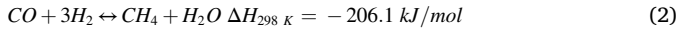
The system analysed in this work uses concentrated solar power (CSP) to decompose methanol (<350 °C) into syngas [49], Fig. 1. Syngas (CO/2H₂) is stored at a pressure of 40 bar and then released to 30 bar in a methanation reactor, where methane (CH_4) and water (H_2O) are produced. Rodriguez-Pastor et al. [50] demonstrated that the overall system yields >40%, obtaining methane mole fractions at the outlet >70% and lower percentages of syngas and water, which can be separated using a flash separator. The obtained gas mixture is a fuel with a high calorific value and flammability that can be stored conventionally in tanks or taken directly into the combustion chamber of a gas turbine.

Fig. 2 illustrates the integration of power generation using a methane/syngas mixture at the outlet of the methanation reactor. In addition to green chemical fuel, power generation can also be provided by the exothermic heat generated in the methanation reactor, for which the operating conditions must be considered to maximise the expelled heat. In both cases, the decomposition and synthesis processes were thermally integrated from a network of heat exchangers to improve the system's overall efficiency and reduce the consumption of hot and cold utilities.

The system comprises four stages, as shown in Fig. 3. The decomposition phase pumps liquid methanol from the storage tank (Stream m10). The liquid methanol is heated from the synthesis gas stream generated in the reactor at a pressure of 40 bar and high temperature. Two-phase methanol enters the decomposition reactor, where the reaction occurs at 315 °C and 10 bar, ensuring a stream of >95% methanol. The remaining excess methanol is separated using a flash separator and recirculated to the main methanol feed stream (Stream 8). The syngas generated in the reactor is transferred to a high-pressure storage tank at temperatures 300 °C.

During the discharge process, it passes through a heat exchanger network (Stream 12), which is heated by the outlet stream of the methanation reactor (18–19). Its pressure is also reduced, and the power obtained in the turbines reduces the associated compressor consumption in the decomposition phase. The process output stream 23 separates
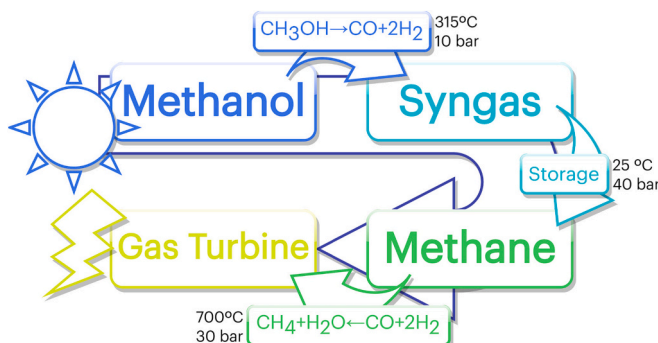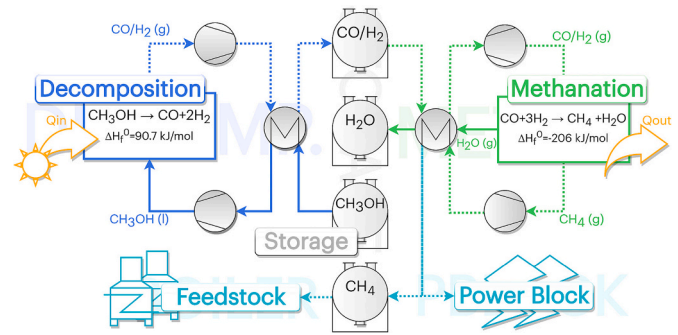

Fig. 2. MeOH-CH₄ thermochemical storage system flowchart.

water from the gaseous mixture, storing the resulting compounds. The resulting fuel is fed into the combustion chamber of a gas turbine (stream 28) to recover energy as electricity. Detailed process streams data are provided in the Annex Section.

Syngas has many applications, from chemical synthesis to power production [51]. Integrated Gasification Combined Cycle (IGCC) technology with carbon capture is a promising solution to achieve high efficiency and reduce pollutant emissions [52]. Hydrogen and carbon monoxide compositions can vary depending on the gasification method, and feedstock used [53]. This variation in composition can affect the combustion performance and application, with much of the research on premixed combustion examining the effects of hydrogen content on ignition, flame structure, laminar flame speed, and syngas NO_x emissions [54–56]. The chemical mechanism of hydrogen appears to be the most significant factor influencing the combustion characteristics of syngas [57]. The flame structure and speed are also strongly influenced by diluent gases, which depend on the syngas composition [58]. In non-premixed combustion, the primary concerns are the effects of syngas composition, strain rate, and diluent gases on flame structure, flammability, and NO_x emissions with counterflow syngas diffusion flames, with or without dilution, which are the main research topics [59]. In this case, the gas turbine operates with a mixture of methane and synthesis gas in its combustion chamber, which helps reduce CO_2 emissions, given a higher H_2 content not synthesised in the methanation reactor [60]. Methane within syngas reduces the maximum flame temperature, resulting in a notable decrease in the production of nitric oxides [61].

3. Modelling

The proposed system was simulated using the commercial software ASPEN HYSYS and Peng–Robinson thermodynamic package. The operating conditions are listed in Table 1.

The system was modelled in a quasi-steady-state manner, considering the concept of peak sun hours (1 kWh/m2), during which the system operates at the design point in the charging phase (Table 2). For the studied location (Seville, Andalusia, Southern Spain), the annual average peak sun hours are approximately 6, resulting in 2190 h of full-load operation per year. The storage tanks were sized to meet the assumed ten hours of discharge for the system to cover three complete discharge cycles (30h), providing backup power production for the gas turbine. The off-design gas turbine conditions owing to weather and load variations were modelled using the commercial software THERMOFLEX [62].

A thermodynamic evaluation was performed based on the definition of the overall performance (η_{plant}) of the TCES/GT system (Eq. (3)).

Fig. 1. Block diagram of the proposed TCES-GT system.

$$\eta_{plant} = \frac{\dot{W}_{GT}}{\dot{Q}_{CH_3OH} + \dot{Q}_{sol}} \cdot \psi = \frac{\dot{W}_{GT}}{HHV_{CH_3OH} \cdot \dot{m}_{CH_3OH} + \dot{W}_{PV} + \dot{Q}_{CSP}} \frac{h_{dis}}{h_{charge}} \tag{3}$$

where $\dot{W}_{GT}$ represents the gas turbine output power, ψ the ratio of discharge (h_{dis}) and charge-storage hours (h_{charge}), HHV_{CH_3OH} and $\dot{m}_{CH_3OH}$
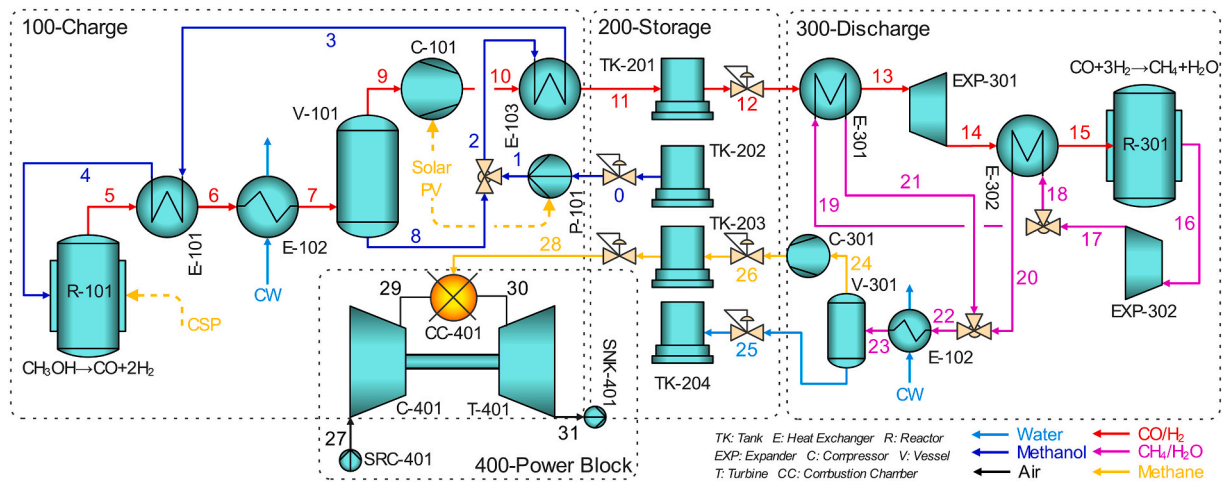
Fig. 3. Proposed MeOH-CH$_4$ thermochemical storage system process flow diagram.

Table 1
Thermodynamic and operational considerations for the proposed system.

Variable	Value
Inlet CH$_3$OH molar flow at the charging process	100 mol/s
CH$_3$OH storage temperature/pressure	64.67 °C/1 bar
Heat Exchangers approach temperature	20 K
Isentropic efficiency of liquid methanol pump	65%
Isentropic efficiency of compressors	89%
Isentropic efficiency of expanders	92%
Endothermic reaction temperature/pressure	315 °C/10 bar
Exothermic reaction temperature/pressure	700 °C/30 bar
Syngas CO/H$_2$ storage pressure	40 bar
Discharge pressure	1 bar
Discharge phase time	10 h

Table 2
Assumptions for meteorological conditions in the model at the design point.

Variable	Value
Ambient Dry Temperature	25 °C
Ambient Pressure	1.013 bar
Location	Seville
Latitude/Longitude	37.383/−5.973
Peak sun hours (PSH)	5.98 (kWh/m^2)

the higher heating value and mass flow rate of methanol, $\dot{W}_{PV}$ the electrical output power of the photovoltaic field and $\dot{Q}_{CSP}$ the thermal output at the receiver of the concentrating solar field.

Thermal performance η_{th} assesses the thermal capacity of the discharge phase from the perspective of the produced fuel ($HHV_{CH_4} \cdot \dot{m}_{CH_4}$) and the exothermic heat ($\dot{Q}_{exo}$) of the methanation reaction, considering the solar input ($\dot{Q}_{sol}$) and methanol contribution ($HHV_{CH_3OH} \cdot \dot{m}_{CH_3OH}$) in the charging phase (Eq. (4)).

$$\eta_{th} = \frac{\dot{Q}_{CH_4} + \dot{Q}_{exo}}{\dot{Q}_{CH_3OH} + \dot{Q}_{sol}} \cdot \psi = \frac{HHV_{CH_4} \cdot \dot{m}_{CH_4} + \dot{Q}_{exo}}{HHV_{CH_3OH} \cdot \dot{m}_{CH_3OH} + \dot{W}_{PV} + \dot{Q}_{CSP}} \cdot \frac{h_{dis}}{h_{charge}} \quad (4)$$

The roundtrip efficiency (RTE) considers the discharge phase electricity output (E_{dis}^{ele}) when considering the charge phase inputs (Eq. (5)).

$$RTE = \frac{E_{dis}^{ele}}{E_{char}} \quad (5)$$

Chemical conversion (η_{sol-ch}) is described by the solar-to-chemical efficiency in terms of power (Eq. (6)).

$$\eta_{sol-ch} = \frac{X_{CH_3OH} \dot{m}_{CH_3OH} \Delta h_{CH_3OH}}{\dot{Q}_{CSP}} \quad (6)$$

where X_{CH_3OH} and Δh_{CH_3OH} are the molar fraction and enthalpy change of methanol, respectively. Finally, the electrical recovery in the discharge-phase expanders was quantified (Eq. (7)) using the solar-to-electrical efficiency ($\eta_{sol-elec}$) as a function of storage time.

$$\eta_{sol-elec} = \frac{\dot{W}_{exp}}{\dot{Q}_{CSP} + \dot{W}_{PV}} \cdot \frac{h_{dis}}{h_{charge}} \quad (7)$$

The proposed system can accommodate various commercial gas turbines such as SIEMENS V93, V94.3, and SGT5-2000E [63] that can handle syngas-based fuels. In this work, the gas turbine selection is determined to provide flexibility in operation, the capability of operating in both simple and combined cycle configurations and versatility of the fuel input in the combustion chamber. SGT-750 gas turbine has been selected for the analysis of the proposed system because of the power range and SNG operation capabilities. SGT-750 main characteristics are provided in Table 3.

Economic analysis depends on the development of the component and product markets, which can affect the accuracy of the approximations used to estimate emerging technologies. The expressions presented in Table 4 form the basis of the economic analysis from the regression of commercial equipment costs as a function of different scaling parameters. Methanol production price was obtained considering renewable biomass sources, considering an average (USD 490/t) based on IRENA analysis (USD 327–764/t) [64].

The estimated costs of the equipment and their influence on the total CAPEX of the facility are shown in Fig. 4. The highest system costs are attributed to the gas turbine (37%) and reactors (~40%), followed by the storage tanks (7%). Due to the integration of the reactor within the CSP receiver tower, the CSP field has a low percentage of the total

Table 3
SGT-750 rated operation for simple cycle power generation.

Parameter	Value
Gross power output	39.8 MW(e)
Gross efficiency	40.3%
Gross heat rate	8922 kJ/kWh
Pressure ratio	24.3: 1
Exhaust temperature	468 °C
Fuel	Natural gas, other gases within specification, liquid fuel (Diesel No. 2) and dual fuel (gas and liquid)

Table 4

Mathematical expressions for estimating the equipment costs.

Equipment	Scaling Parameter	Expression	Ref.
Compressors	Power (kW)	$IC_C = 643.15 \bullet \dot{W}_C^{0.9142}$	[65]
Expanders	Power (kW)	$IC_{exp} = 4001.4 \bullet \dot{W}_{exp}^{0.6897}$	[66]
Pump	Power (kW) and pump efficiency (−)	$IC_P = 3531.4 \bullet \dot{W}_P^{0.71} \bullet \left[1 + \left(\frac{1 - 0.8}{1 - \eta_{i,P}} \right)^3 \right]$	[67]
Heat Exchangers	Area (m^2) and pressure (bar)	$IC_{HE} = 2546.9 \bullet A_{HE}^{0.67} \bullet P_{HE}^{0.28} \bullet 10^{-6}$	[67]
Air Cooler	Cooling power (kW)	$IC_{Cooling}^{tower} = 32.3 \bullet \dot{Q}_{cool}$	[68]
Endothermic Reactor	Thermal power (kW)	$IC_{Dr} = 13140 \bullet \dot{Q}_r^{0.67}$	[69]
Exothermic Reactor	Thermal power (kW)	$IC_{Mr} = 19594 \bullet \dot{Q}_r^{0.5}$	[69]
Tanks	Volume (m^3)	$IC_{Tank} = 83 \bullet V_{tank}$	[70]
Solar PV Field	Power (kW)	$IC_{PV} = 0.995 \bullet \dot{W}_{PV} \bullet 10^3$	[71]
CSP Field	Receiver thermal power (kW)	$IC_{rec}^{solar} = 57.07 \bullet \Phi_{Receiver}$	[72]
Gas Turbine	Net GT power (kW)	$IC_{GT} = 8279 \bullet W_{GT}^{0.6842}$	[73]
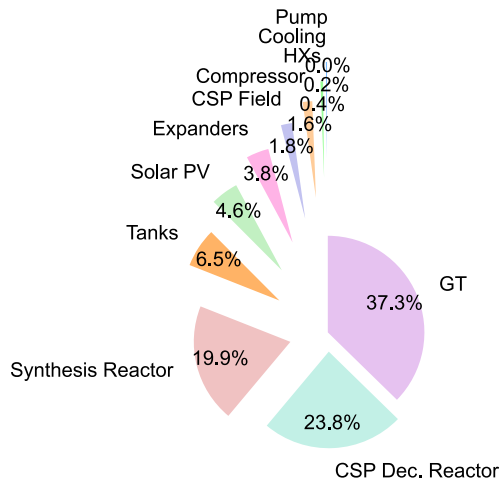
Fig. 4. Influence of estimated component costs on total capital expenditures (CAPEX) of the proposed facility.

capital expenditures (2%).

The levelized cost of fuel (LCOF) and levelized cost of energy (LCOE) indicators are proposed for the overall economic evaluation (Eqs. (8) and (9)), considering a discount rate (*r*) of 5%, useful life of the plant (*n*) of 20 years.

$$LCOF = \frac{CAPEX + \sum_{i=1}^{n} \frac{OPEX_i}{(1+r)^i}}{\sum_{i=1}^{n} \frac{E_{fuel}}{(1+r)^i}} \qquad (8)$$

CAPEX being the initial investment cost of the plant, $OPEX_i$ is the annual operation and maintenance cost and $E_{fuel} = \dot{m}_{fuel} LHV_{fuel} \frac{h_{dis}}{year}$ the annual fuel energy produced in the discharge phase of the proposed system (MWh).

$$LCOE = \frac{CAPEX + \sum_{i=1}^{n} \frac{OPEX_i}{(1+r)^i}}{\sum_{i=1}^{n} \frac{E_{GT}}{(1+r)^i}} \qquad (9)$$

and E_{GT} the annual energy produced in the bottoming gas turbine cycle

in MWh. Applying the same concept, the levelized cost of storage (LCOS) is shown in Eq. (10):

$$LCOS = \frac{CAPEX + \sum_{i=1}^{n} \frac{OPEX_i}{(1+r)^i}}{\sum_{i=1}^{n} \frac{m_{dis} \Delta h_{dis}}{(1+r)^i}} \qquad (10)$$

4. Results and discussion

Table 5 evaluates the efficiencies mentioned earlier based on the proposed operating parameters resulting from the techno-economic optimisation of the involved processes.

The high solar-to-chemical efficiency is noteworthy because of the low-temperature requirement of the methanol decomposition process. This effect is also reflected in the solar-to-electric efficiency, which indicates the associated conversion of solar irradiation to electricity in terms of power, reaching 14.4%. The overall efficiency of the plant, which evaluates the power generation in the gas turbine and associated storage considering the power generation in the discharge phase expanders, is 28.9%, representing a competitive value in terms of energy conversion efficiency. This is conditioned by thermal efficiency and gas turbine efficiency, with the former reaching 51.1%, which is highly influenced by the temperature of the discharge-phase reaction (methanation). The gas turbine efficiency is affected by the molar fraction at the reactor outlet, which increases as the methane yield increases, negatively impacting the CO_2 emissions, as discussed. A round trip efficiency (RTE) of around 44% is achieved, which falls within the obtained values (47%) for a hydrogen system using 350 bar compressed gas storage [74]. This indicates that the proposed system is competitive from the perspective of electrical energy storage and offers advantages compared with green hydrogen installations, such as lower transportation costs, lower operating pressure, and greater flexibility in the processes, which can be effectively integrated into existing industries.

A levelized cost of fuel value of €172.44/MWh was obtained from techno-economic optimisation, which is lower in agreement with those reported in other studies owing to the improved thermal integration of equipment and a reduction in compression costs. Obtaining low-cost biomass at the output level implies lower costs than, for example, those reported by Götz et al. [75] for SNG currently (€165–392/MWh), of the same order (€90–115/MWh) for green ammonia [76], and higher than that of green ethanol using lignocellulosic biomass in Europe (€60–100/MWh) [77]. In the proposed system, the levelized cost of energy (LCOE) resulting from power generation in the gas turbine was €261.14/MWh, which may be competitive (<€200/MWh) as the cost of green biomethanol production decreases (<€390/t) according to IRENA predictions [64], as will be discussed. Compared to other technologies, the proposed system can be competitive, offering high flexibility and long-term storage. Badouard et al. [78] reported an LCOE for concentrated solar power ranged between €69–234/MWh and €108–€225/MWh for solid biomass-fired power plants. In gas turbines and combined

Table 5

Overall performance and thermodynamic conversion efficiency of the proposed system.

Parameter	Value
Solar-to-chemical efficiency (η_{sol-ch})	0.665
Solar-to-electrical efficiency ($\eta_{sol-elec}$)	0.144
Overall performance (η_{plant})	0.289
Thermal efficiency (η_{th})	0.511
Roundtrip efficiency (RTE)	0.438
Required endothermic reaction heat [MW] ($\dot{Q}_{CSP}$)	12.841
Exothermic reaction heat [MW] ($\dot{Q}_{exo}$)	7.57
CAPEX [M€]	32.936
OPEX [€/kW-year]	82.21
LCOF [€/MWh]	172.44
LCOE [€/MWh]	261.14

cycles, ETN Global [79] estimated levelized costs between €141–191/ MWh burning 100% H_2 with a fixed price of €1.5/kg H_2.

4.1. Off-design considerations

Different strategies can be used for operating under gas turbine variable load conditions [80]. The most common approaches include adjusting the fuel flow, which involves varying the amount of fuel injected into a constant air mass flow rate in the combustor, modifying the compressor geometry (VIGV: Variable Inlet Guide Vanes), and varying the shaft speed in multishaft engines. In practical applications, many gas turbines utilise multiple control systems across their operating range, whether they are used independently or as part of a combined cycle power plant. The impact of these control methods on overall plant efficiency depends largely on the plant layout, as each control approach affects its components differently [80,81].

Fig. 5 compares the proposed gas turbine employing a variable compressor geometry and variable turbine inlet temperature. The former case reduces the air mass flow rate to approximately 65% of its rated value at part-load. In contrast, the combustor's fuel-to-air ratio (FAR) (and consequently, the turbine inlet temperature) remains constant. As the engine pressure ratio decreases at lower airflow rates, this control approach leads to a decrease in efficiency and an increase in the turbine exhaust temperature. To mitigate the adverse effects of higher exhaust temperatures on downstream equipment, some engines that use this strategy may reduce the FAR to maintain a constant exhaust temperature.

In contrast, engines operating at a constant airflow rate experience concurrent reductions in turbine inlet and exhaust temperatures. This simultaneous decrease has a less detrimental impact on efficiency because less heat is rejected to the environment. In other words, the effect of lower temperature dominates over the reduced exhaust flow rate in terms of heat rejection.

4.2. Sensitivity analysis

Elevated thermal efficiencies were achieved in the gas turbine due to the additional carbon monoxide content in the fuel. Various Turbine Inlet Temperatures (TIT) and pressure ratios (PR) were analysed based on the gas turbine technology investigated in this study, reaching a maximum of 45.3% at 1200 °C TIT and a minimum of 33.4% at 1000 °C TIT.

The decomposition temperature of methanol, which is highly dependent on the available solar resources, significantly affects the chemical conversion efficiency, as shown in Fig. 6A. The maximum efficiency was achieved at temperatures between 200 °C and 250 °C, which shifted with temperature as the decomposition pressure increased. In this regard, low temperatures lead to slower kinetics and the need for a greater catalyst amount [83]. The effect on the amount of catalyst is not considered in this work. The decomposition temperature did not significantly affect the overall plant efficiency, as the heat required for the complete conversion of methanol to syngas (<300 °C) increased abruptly and was offset by the exothermic energy generated in the methanation reactor. However, the system's thermal efficiency is affected by the incomplete conversion of methanol, resulting in a lower mass fuel expenditure (methane) during the discharge phase (Fig. 6B). Likewise, the roundtrip efficiency depends on the conversion in the methanation reaction (Fig. 6C), thus requiring complete decomposition (315 °C at 10 bar) to achieve a maximum of 44%, which remains nearly constant with the syngas storage pressure.

In the discharge phase, the efficiency associated with electrical recovery in the turbines (Fig. 7C) improved significantly with the methanation temperature and lower inlet pressures. This was due to the higher enthalpy at the reactor outlet and increased utilisation in the expanders, despite a penalty in the roundtrip and overall plant efficiency, as depicted in Fig. 7A and B. The benefits associated with high temperatures in the methanation reaction, which provide improved costs without significant penalising conversion, have been demonstrated in the industry [47].
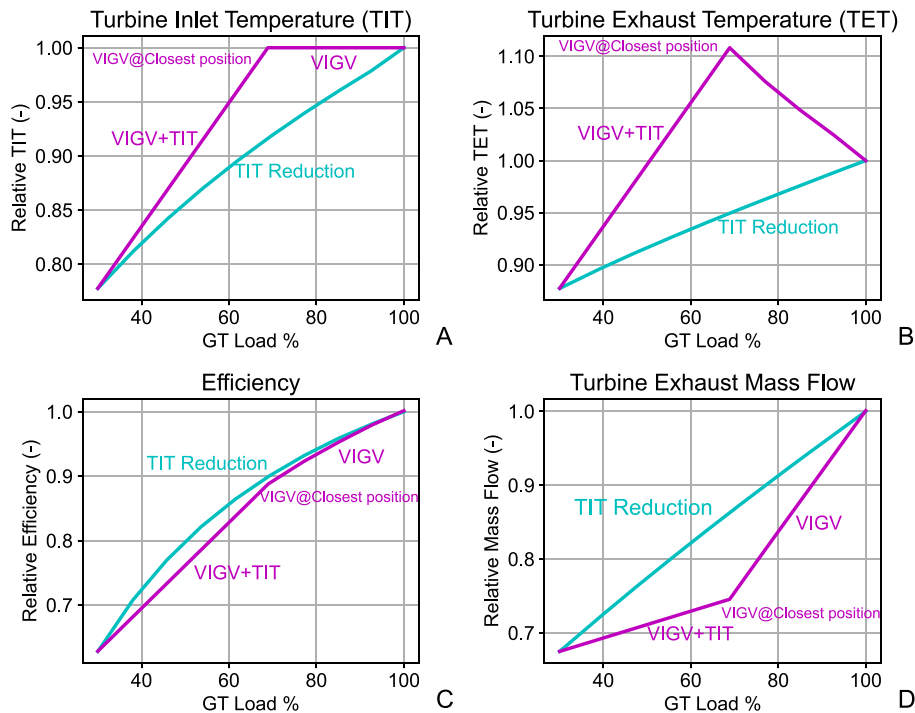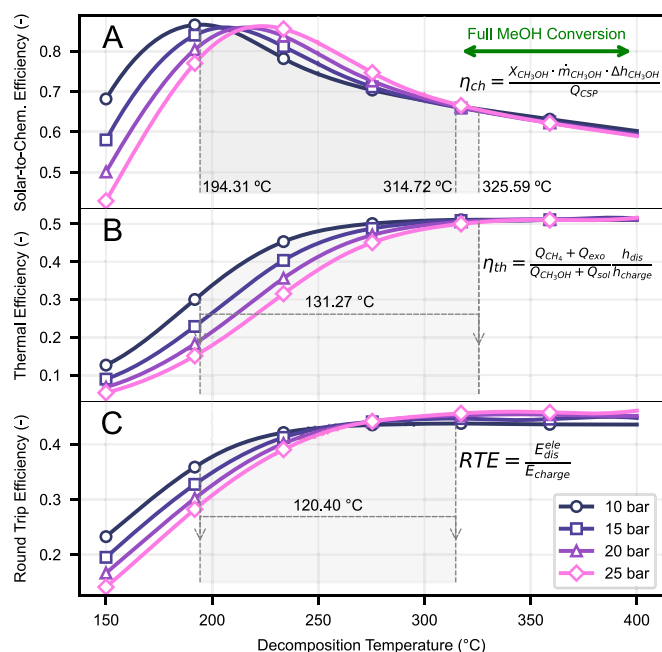

Fig. 5. Simulated THERMOFLEX SGT-750 performance maps. Relative variation of A) Inlet temperature to the turbine (TIT), B) Outlet temperature from the turbine, C) Plant efficiency, D) Mass flow rate at the turbine outlet, as a function of the selected turbine load and strategy (TIT Reduction/VIGV: Variable Inlet Guide Vanes) in the proposed system.

Fig. 6. Variation as a function of direct methanol decomposition reaction temperature at different pressures of A) Solar-to-chemical efficiency B) Thermal efficiency C) Roundtrip efficiency.

As the conversion of hydrogen to methane is the objective for the direct use of this product in gas turbines and the chemical industry, a storage system is preferred at lower reaction temperatures and higher hydrogen conversion, as illustrated in Fig. 8. When operating in a closed cycle, such as methane-to-syngas/syngas-to-methanol, complete conversion in the methanation reaction favours the efficiency of the proposed thermochemical energy storage system. Furthermore, a positive trend was observed as the pressure decreased, favouring a combination of high pressure during the charging phase and low pressure during the discharge process.

The solar-to-electric efficiency increased with the storage pressure, reaching values above 18% for pressures higher than 100 bar, owing to a higher power output from the expanders in the discharge phase. This system is of great interest because methanol can be pumped in a liquid state, leading to significant energy savings in the syngas compression phase. Fig. 9 illustrates that the electrical recovery power indicator (power obtained in the discharge phase, subtracting the power required in the charging process) does not affect the system efficiency to the same

extent.

4.3. Economic analysis

The economic characterisation has been conducted following the mathematical regressions presented in Table 4, assessing the specific cost of each technology based on its scaling parameter. In this work, the overall cost of the installation is estimated as a function of the decomposition and synthesis reactions' thermodynamic parameters (temperature/pressure). Thus, high decomposition pressures favoured facility costs because of the savings associated with methanol pumping instead of syngas compression. Higher methanol decomposition temperatures also resulted in improved energy and fuel costs, obtaining a levelized cost of fuel of €171/MWh at a reaction pressure of 25 bar (Fig. 10A). The same effect is reflected in the levelized cost of storage (LCOS), owing to increased SNG production and the higher equivalent conversion rate in the methanation reactor, Fig. 10C. The levelized cost of energy (LCOE) obtained from the gas turbine is evaluated in Fig. 10B, where the complete conversion of methanol to methane results in lower levelized costs, reaching €256/MWh, owing to the maintained power generated in the turbine (denominator of the function) with decreasing capital costs.

For the nominal charging phase, the economic impact of the fuel costs of the discharging phase is less significant, with only a variation in the levelized cost of energy (LCOE), as shown in Fig. 10E. This is because of the flammable content of hydrogen and carbon monoxide as excess reaction products, which serve as fuel in the combustion chamber of the gas turbine. At the industrial level, higher methanation temperatures ensure lower reactor costs, and in the proposed configuration, higher energy in the methane stream at the outlet ensures a higher turbine power output. This is demonstrated in Fig. 10D and Fig. 10F, where the levelized costs of fuel produced decrease by up to €25/MWh between the higher methanation conversion conditions (200 °C/40 bar) and the assumed operating conditions (700 °C/30 bar), also observed for the LCOS, which decreases by up to €15/MWh.

The cost of green methanol production depends on several factors, such as the availability and price of biomass feedstock, scale and efficiency of gasification and methanol synthesis plants, location and transport costs, and environmental regulations and incentives. In this regard, the estimation of the cost per ton was discussed for integration into the proposed system. According to IRENA, biomethanol prices considering a feedstock price below €5.4/GJ amount to €327/t and €764/t for more expensive feedstock (Fig. 11A). This translates into an equivalent fuel (methane) price in our configuration of €455–1013/t, respectively (Fig. 11B). When considering e-methanol or methanol from electrochemical methods, either with CO_2 and renewables, or CO_2 via direct air capture (DAC), methanol prices are substantially higher,
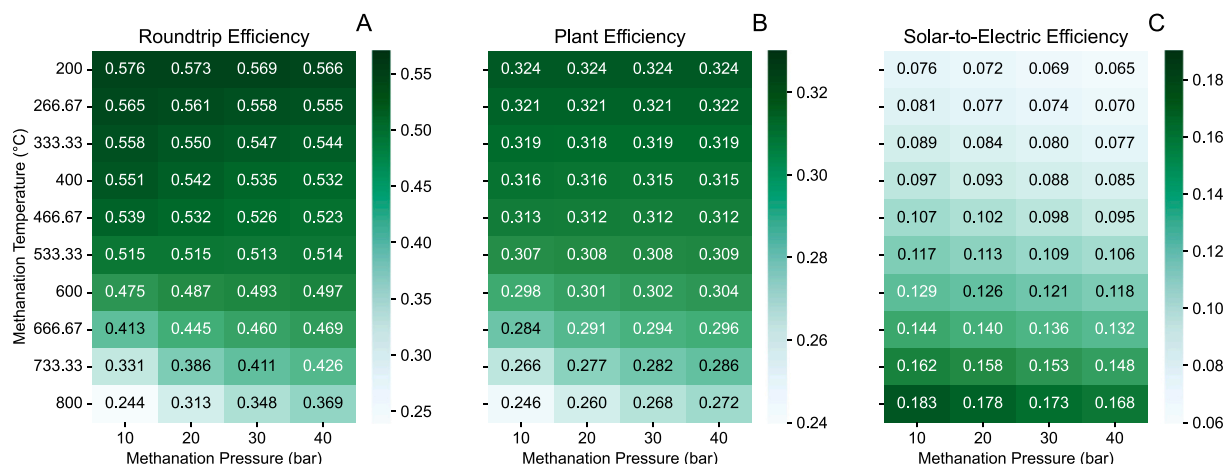
Fig. 7. Variation as a function of methanation reaction temperature of A) Roundtrip efficiency, B) Overall plant performance and C) Solar-to-electric efficiency.
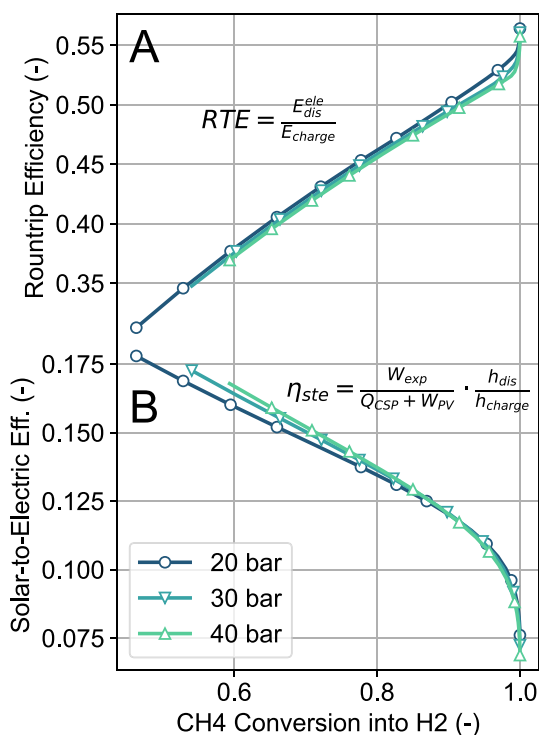
Fig. 8. Variation in storage performance as a function of hydrogen to methane conversion in the methanation reactor.
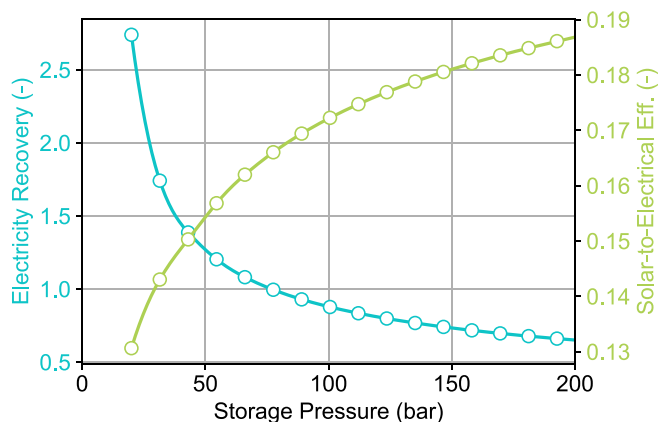

Fig. 9. Change in electrical recovery and solar-to-electrical performance as a function of syngas storage pressure.

ranging from €820–2380/t at present. With these methanol costs, the equivalent fuel obtained ranged from €1024–2832/t. Thus, the minimum LCOE obtained was €187/MWh for low-cost biomass and the maximum was €1118/MWh for e-methanol with DAC. Predictions for higher maturity levels assume biomethanol costs of €227/t, which would decrease the LCOE to €142/MWh. Similarly, in 2050, for a significant production level, the e-methanol cost is expected to fall to €250/t, leading to an LCOE of €152/MWh, at which point the system would be highly competitive.

5. Conclusions

This paper proposes a novel thermochemical storage system based on directly converting methanol to syngas at moderate temperatures (<315 °C) using concentrated solar power and its subsequent synthesis to methane through methanation. The processes involved are well-

known in the chemical industry and have a high level of maturity, where the integration of the studied chemical reactions represents a novelty for flexible power generation in gas turbine systems. The obtained costs were competitive with those of other SNG and green fuel production technologies, with the advantage of having a high volumetric energy density hydrocarbon that can be produced from renewable sources, such as methanol. The following conclusions can be drawn:

- The decomposition temperature of methanol significantly affected the chemical conversion efficiency, achieving maxima at temperatures between 200 and 250 °C and shifting with temperature as the decomposition pressure increased. The decomposition temperature did not significantly affect the overall plant efficiency, resulting in 28.9% for the design point.
- In the discharge phase, the efficiency associated with electrical recovery in the turbines improved significantly with the methanation temperature and lower inlet pressures. High temperatures in the methanation reaction result in improved costs without significant penalising conversion.
- When operating in a closed cycle, complete conversion in the methanation reaction (200–400 °C) does not improve the efficiency of the thermochemical storage system (44%). A positive trend was observed from the combination of high pressure during the charging phase (<40 bar) and low pressure during the discharging phase (<20 bar).
- The complete conversion of methanol to methane decreases the levelized costs owing to the maintained power generated in the turbine with reduced capital costs. Higher methanol decomposition temperatures improved energy and fuel costs, reaching €256/MWh and €171/MWh, respectively.
- Biomethanol prices amounted to €327/t and €764/t for more expensive feedstock, implying an equivalent fuel (methane) price in proposed configuration of €124–254/MWh. When considering e-methanol prices, the obtained prices range from €162–329/MWh.
- The minimum LCOE obtained is €187/MWh for low-cost biomass and €1118/MWh for e-methanol with DAC. Predictions for higher maturity levels assume biomethanol costs of €254/t, decreasing the LCOE to €142/MWh. Costs of e-methanol are expected to fall to €250/MWh, leading to an LCOE of €152/MWh, at which point the system would be highly competitive.

Authors' contributions

D.A Rodriguez-Pastor: Conception and design of the study, Acquisition of data, Analysis and/or interpretation of data, Simulation, Writing - original draft. *A. Garcia-Guzman:* Simulation, Analysis and/or interpretation of data. *C. Ortiz:* Conception and design of the study, Analysis and/or interpretation of data, Writing - original draft. *E. Carvajal*: Analysis and/or interpretation of data. *J.A Becerra:* Conception and design of the study, Analysis and/or interpretation of data, Writing - review & editing. *V.M Soltero:* Analysis and/or interpretation of data, Writing - review & editing. *R. Chacartegui:* Conception and design of the study, Analysis and/or interpretation of data, Writing - original draft - review & editing.

CRediT authorship contribution statement

D.A. Rodriguez-Pastor: Writing – original draft, Software, Investigation, Data curation, Conceptualization. **A. Garcia-Guzman:** Software, Investigation, Conceptualization. **I. Marqués-Valderrama:** Software, Investigation, Conceptualization. **C. Ortiz:** Writing – review & editing, Validation, Investigation, Data curation, Conceptualization. **E. Carvajal:** Data curation. **J.A. Becerra:** Writing – review & editing, Investigation, Data curation, Conceptualization. **V.M. Soltero:** Writing – review & editing, Supervision. **R. Chacartegui:** Writing – review & editing, Validation, Supervision, Methodology, Formal analysis,
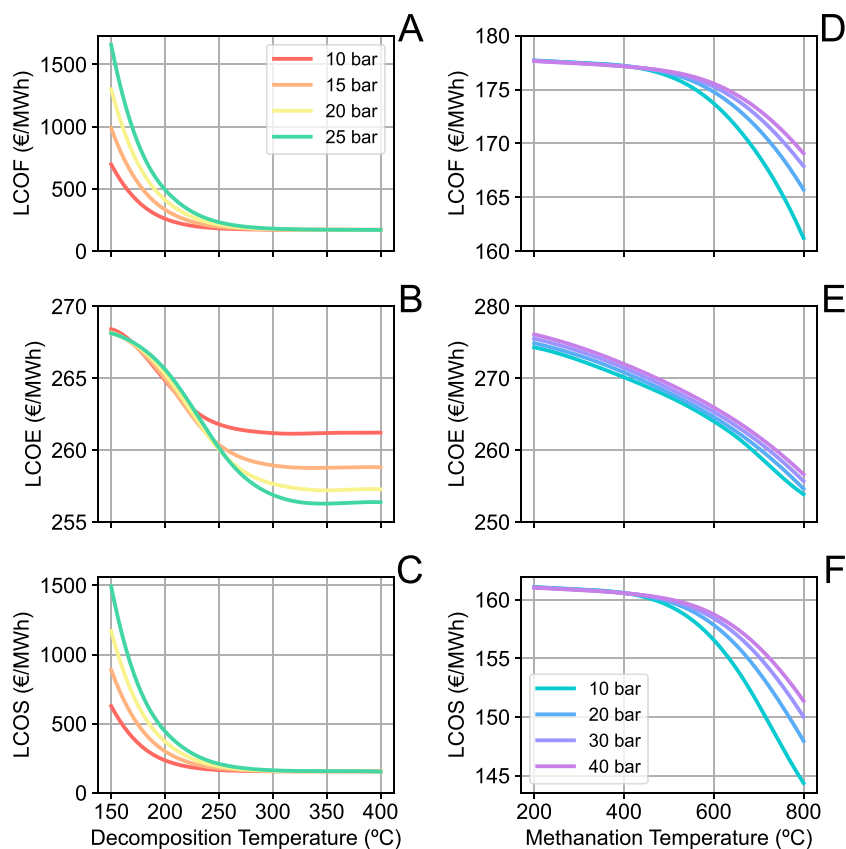
Fig. 10. A) Levelized cost of fuel, LCOF in €/MWh, B) levelized cost of energy, LCOE in €/MWh, and C) levelized cost of storage, LCOS in €/MWh, as a function of direct methanol decomposition temperature. D) Levelized cost of fuel, LCOF in €/MWh, E) levelized cost of energy, LCOE in €/MWh, and F) levelized cost of storage, LCOS in €/MWh, as a function of methanation temperature.
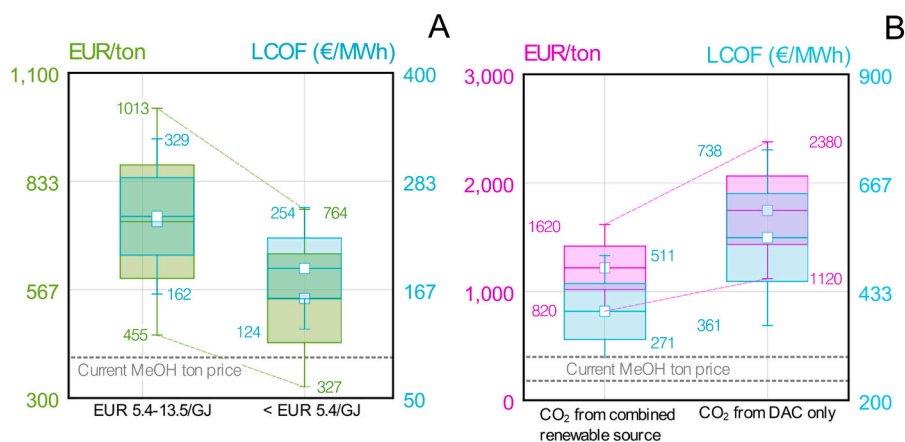
Fig. 11. Predicted costs per ton of fuel produced by the proposed system based on A) methanol from biomass (based on feedstock cost) and B) e-methanol from CO_2 from a combined renewable source and Direct Air Capture (DAC). Methanol price data from [64].

Conceptualization.

Declaration of Competing Interest

The authors declare that they have no known competing financial interests or personal relationships that could have appeared to influence the work reported in this paper.

Data availability

Data will be made available on request.

Annex A

Streams main data for the proposed installation.

Stream	Temperature (°C)	Pressure (bar)	Molar Flow (kmol/h)	Mass Flow (kg/h)	Mass Enthalpy (kJ/kg)	Mass Entropy (kJ/kg-K)
0	25.00	0.14	360.00	11,535.08	−7549.02	0.51
1	25.00	0.14	360.00	11,535.08	−7549.02	0.51
2	25.17	10	360.00	11,535.08	−7547.34	0.51
3	134.11	10	360.00	11,535.08	−7131.93	1.69
4	139.20	10	360.00	11,535.08	−6691.12	2.76
5	315.00	10	1074.96	11,535.44	−2683.49	13.15
6	154.11	10	1074.96	11,535.44	−3124.29	12.28
7	30.00	10	1074.96	11,535.44	−3351.75	11.69
8	30.00	10	2.52	80.70	−7530.40	0.57
9	30.00	10	1072.44	11,454.74	−3439.53	11.39
10	197.72	40	1072.44	11,454.74	−2983.92	11.50
11	45.17	40	1072.44	11,454.74	−3402.24	10.43
12	45.17	40	1072.44	11,454.74	−3402.24	10.43
13	119.19	40	1072.44	11,454.74	−3199.42	11.00
14	90.33	30	1072.44	11,454.74	−3277.85	11.02
15	145.92	30	1072.44	11,454.74	−3126.04	11.41
16	700.00	30	671.36	11,454.56	−5505.44	11.29
17	256.89	1.00	671.36	11,454.56	−6592.18	11.48
18	256.89	1.00	335.68	5727.28	−6592.18	11.48
19	256.89	1.00	335.68	5727.28	−6592.18	11.48
20	110.33	1.00	335.68	5727.28	−6895.82	10.81
21	68.53	1.00	335.68	5727.28	−6997.83	10.52
23	84.44	1.00	671.36	11,454.56	−6946.81	10.67
24	60.00	1.00	671.36	11,454.56	−7305.68	9.61
25	60.00	1.00	588.05	9953.72	−6034.45	10.54
26	60.00	1.00	83.31	1500.84	−15,736.66	3.46
27	25.00	1.013	13,975.61	403,200.00	−0.28	5.26
28	476.15	24.30	588.05	9953.72	−5115.36	10.73
29	476.53	24.0	13,975.61	403,200.00	478.14	5.31
30	1100.00	24.0	14,428.37	413,152.83	525.82	6.22
31	414.78	1.013	14,428.37	413,152.83	−288.41	6.33

References

[1] Kousksou T, Bruel P, Jamil A, El Rhafiki T, Zeraouli Y. Energy storage: applications and challenges. Solar Energy Mater Solar Cells 2014;120:59–80. https://doi.org/10.1016/J.SOLMAT.2013.08.015.

[2] Koytsoumpa EI, Bergins C, Buddenberg T, Wu S, Sigurbjörnsson Ó, Tran KC, et al. The challenge of Energy storage in Europe: focus on power to Fuel. J Energy Resourc Technol Trans ASME 2016:138. https://doi.org/10.1115/1.4032544/373064.

[3] Ortiz C, Chacartegui R, Valverde JM, Alovisio A, Becerra JA. Power cycles integration in concentrated solar power plants with energy storage based on calcium looping. Energ Conver Manage 2017;149:815–29. https://doi.org/10.1016/J.ENCONMAN.2017.03.029.

[4] KlinSoda I, Piumsomboon P. Isopropanol–acetone–hydrogen chemical heat pump: a demonstration unit. Energ Conver Manage 2007;48:1200–7. https://doi.org/10.1016/J.ENCONMAN.2006.10.006.

[5] Kyaw K, Matsuda H, Hasatani M. Applicability of carbonation/Decarbonation reactions to high-temperature thermal Energy storage and temperature upgrading. J Chem Eng Japan 1996;29:119–25. https://doi.org/10.1252/JCEJ.29.119.

[6] Criado JM, Macias M, Macias-Machín A. Analysis of the system CaO-CO2-H2O for storage of solar thermal energy. Solar Energy 1992;49:83–6. https://doi.org/10.1016/0038-092X(92)90141-V.

[7] Kato Y, Yamashita N, Kobayashi K, Yoshizawa Y. Kinetic study of the hydration of magnesium oxide for a chemical heat pump. Appl Therm Eng 1996;16:853–62. https://doi.org/10.1016/1359-4311(96)00009-9.

[8] Dunn R, Lovegrove K, Burgess G. A review of ammonia-based thermochemical energy storage for concentrating solar power. Proc IEEE 2012;100:391–400. https://doi.org/10.1109/JPROC.2011.2166529.

[9] McCrary JH, McCrary GE, Chubb TA, Won YS. An experimental study of SO3 dissociation as a mechanism for converting and transporting solar energy. Solar Energy 1981;27:433–40. https://doi.org/10.1016/0038-092X(81)90008-6.

[10] Liu Q, Yabe A, Kajiyama S, Fukuda K. A review of study on thermal energy transport system by synthesis and decomposition reactions of methanol. JSME Int J Ser B: Fluids Therm Eng 2002;45:473–80. https://doi.org/10.1299/JSMEB.45.473.

[11] Chen X, Zhang Z, Qi C, Ling X, Peng H. State of the art on the high-temperature thermochemical energy storage systems. Energ Conver Manage 2018;177:792–815. https://doi.org/10.1016/J.ENCONMAN.2018.10.011.

[12] IEA. Renewable methanol. 2021.

[13] Gautam P, Upadhyay S, Fuel SD. Bio-methanol as a renewable fuel from waste biomass: Current trends and future perspective. Elsevier; 2020.

[14] ChemCatChem MB. Methanol synthesis from CO2 hydrogenation11. Wiley Online Library 2019; 2019. p. 4238–46. https://doi.org/10.1002/cctc.201900401.

[15] Räuchle K, Plass L, Wernicke HJ, Bertau M. Methanol for renewable Energy storage and utilization. Energ Technol 2016;4:193–200. https://doi.org/10.1002/ENTE.201500322.

[16] Garcia G, Arriola E, Chen WH, De Luna MD. A comprehensive review of hydrogen production from methanol thermochemical conversion for sustainability. Energy 2021;217:119384. https://doi.org/10.1016/J.ENERGY.2020.119384.

[17] Ashurst J, Nappe T. Methanol toxicity. 2018.

[18] Review DS-JMT. Methanol production-a technical history. Technology Matthey Com; 2017.

[19] Carapellucci R, Risalvato V, Bruno C, Cau G. Performance and emissions of CRGT power generation systems with reformed methanol. Proc Intersoc Energy Conv Eng Conf 1996;2:707–12. https://doi.org/10.1109/IECEC.1996.553784.

[20] Tola V, Lonis F. Low CO2 emissions chemically recuperated gas turbines fed by renewable methanol. Appl Energy 2021;298:117146. https://doi.org/10.1016/J.APENERGY.2021.117146.

[21] Cherednichenko O, Havrysh V, Shebanin V, Kalinichenko A, Mentel G, Nakonieczny J. Local green power supply plants based on alcohol regenerative gas turbines: economic and environmental aspects. Energies (Basel) 2020;13. https://doi.org/10.3390/EN13092156.

[22] Poullikkas A. An overview of current and future sustainable gas turbine technologies. Renew Sustain Energy Rev 2005;9:409–43. https://doi.org/10.1016/j.rser.2004.05.009.

[23] Moioli E, Mutschler R, Züttel A. Renewable energy storage via CO2 and H2 conversion to methane and methanol: assessment for small scale applications. Renew Sustain Energy Rev 2019;107:497–506. https://doi.org/10.1016/J.RSER.2019.03.022.

[24] Garcia G, Arriola E, Chen WH, De Luna MD. A comprehensive review of hydrogen production from methanol thermochemical conversion for sustainability. Energy 2021;217:119384. https://doi.org/10.1016/J.ENERGY.2020.119384.

[25] Biswas S, Kulkarni AP, Giddey S, Bhattacharya S. A review on synthesis of methane as a pathway for renewable energy storage with a focus on solid oxide electrolytic cell-based processes. Front Energy Res 2020;8:229. https://doi.org/10.3389/FENRG.2020.570112/BIBTEX.

[26] Haynes CA, Gonzalez R. Rethinking biological activation of methane and conversion to liquid fuels. Nat Chem Biol 2014;10(5):331–9. https://doi.org/10.1038/nchembio.1509.

[27] Dieterich V, Buttler A, Hanel A, Spliethoff H, Fendt S. Power-to-liquid via synthesis of methanol, DME or Fischer–Tropsch-fuels: a review. Energ Environ Sci 2020;13:3207–52. https://doi.org/10.1039/D0EE01187H.

[28] Edlund D, Lim D. The renewable methanol pathway to green hydrogen. Methanol Institute; 2021.

[29] Dieterich V, Buttler A, Hanel A, Spliethoff H, Fendt S. Power-to-liquid via synthesis of methanol, DME or Fischer–Tropsch-fuels: a review. Energ Environ Sci 2020;13:3207–52. https://doi.org/10.1039/D0EE01187H.

[30] Bai Z, Liu Q, Lei J, Energy HJ-A. Investigation on the mid-temperature solar thermochemical power generation system with methanol decomposition. Elsevier; 2018.

[31] Liu T, Bai Z, Zheng Z, Liu Q, Lei J, Sui J, et al. 100 kWe power generation pilot plant with a solar thermochemical process: design, modeling, construction, and

testing. Appl Energy 2019;251:113217. https://doi.org/10.1016/J. APENERGY.2019.05.020.

[32] Ranjekar AM, Yadav GD. Steam reforming of methanol for hydrogen production: a critical analysis of catalysis, processes, and scope. Ind Eng Chem Res 2021;60: 89–113. https://doi.org/10.1021/ACS.IECR.0C05041/SUPPL_FILE/IE0C05041_SI_001.PDF.

[33] Pastore L, Basso G, Energy L de S. Can the renewable energy share increase in electricity and gas grids takes out the competitiveness of gas-driven CHP plants for distributed generation? Elsevier; 2022.

[34] Sorknæs P, Lund H, Skov I, Djørup S, Reviews KS-… E. Smart energy markets-future electricity, gas and heating markets. Elsevier; 2020.

[35] Skorek-Osikowska A, Martín-Gamboa M, Dufour J. Thermodynamic, economic and environmental assessment of renewable natural gas production systems. Energy Convers Managem X 2020;7:100046. https://doi.org/10.1016/J. ECMX.2020.100046.

[36] Gassner M, Maréchal F. Thermo-economic process model for thermochemical production of synthetic natural gas (SNG) from lignocellulosic biomass. Biomass Bioenergy 2009;33:1587–604. https://doi.org/10.1016/J. BIOMBIOE.2009.08.004.

[37] Gassner M, Maréchal F. Thermo-economic optimisation of the polygeneration of synthetic natural gas (SNG), power and heat from lignocellulosic biomass by gasification and methanation. Energ Environ Sci 2012;5:5768–89. https://doi.org/10.1039/C1EE02867G.

[38] Uchman W, Skorek-Osikowska A, Jurczyk M, Węcel D. The analysis of dynamic operation of power-to-SNG system with hydrogen generator powered with renewable energy, hydrogen storage and methanation unit. Energy 2020;213: 118802. https://doi.org/10.1016/J.ENERGY.2020.118802.

[39] Toro C, Sciubba E. Sabatier based power-to-gas system: Heat exchange network design and thermoeconomic analysis. 2018. https://doi.org/10.1016/j. apenergy.2018.08.036.

[40] CRC Handbook of Chemistry and Physics. CRC Handbook of Chemistry and Physics. 2016. https://doi.org/10.1201/9781315380476.

[41] Schorn F, Breuer JL, Samsun RC, Schnorbus T, Heuser B, Peters R, et al. Methanol as a renewable energy carrier: an assessment of production and transportation costs for selected global locations. Adv Appl Energy 2021;3:100050. https://doi. org/10.1016/J.ADAPEN.2021.100050.

[42] Chacartegui Ramírez R, Ja Becerra Villanueva, Jm Valverde Millán, Ortiz Domínguez C, Masci G. ES2792748B2 - Instalacion de almacenamiento de energia termoquimicamecanica y procedimiento de almacenamiento de energia. 2019.

[43] Poudel J, Choi JH, Oh SC. Process design characteristics of syngas (CO/H2) separation using composite membrane. Sustainability 2019;11:703. https://doi. org/10.3390/SU11030703.

[44] Mauri S, D'Olimpio G, Ghica C, Braglia L, Kuo C-N, Istrate MC, et al. Hydrogen Production mechanism in low-temperature methanol decomposition catalyzed by Ni3Sn4 intermetallic compound: a combined operando and density functional theory investigation. J Phys Chem Lett 2023;14:1334–42. https://doi.org/10.1021/ACS.JPCLETT.2C03471.

[45] Cheng WH. Reaction and XRD studies on cu based methanol decomposition catalysts: role of constituents and development of high-activity multicomponent catalysts. Appl Catal Gen 1995;130:13–30. https://doi.org/10.1016/0926-860X (95)00102-6.

[46] Gao J, Wang Y, Ping Y, Hu D, Xu G, Gu F, et al. A thermodynamic analysis of methanation reactions of carbon oxides for the production of synthetic natural gas. RSC Adv 2012;2:2358–68. https://doi.org/10.1039/C2RA00632D.

[47] Rönsch S, Schneider J, Matthischke S, Schlüter M, Götz M, Lefebvre J, et al. Review on methanation – from fundamentals to current projects. Fuel 2016;166:276–96. https://doi.org/10.1016/J.FUEL.2015.10.111.

[48] Zhang Z, Tian Y, Zhang L, Hu S, Xiang J, Wang Y, et al. Impacts of nickel loading on properties, catalytic behaviors of Ni/γ–Al2O3 catalysts and the reaction intermediates formed in methanation of CO2. Int J Hydrogen Energy 2019;44: 9291–306. https://doi.org/10.1016/J.IJHYDENE.2019.02.129.

[49] Bai Z, Liu Q, Gong L, Lei J. Application of a mid−/low-temperature solar thermochemical technology in the distributed energy system with cooling, heating and power production. Appl Energy 2019;253:113491. https://doi.org/10.1016/J. APENERGY.2019.113491.

[50] Rodriguez-Pastor DA, Carro A, Masci G, Ortiz C, Verda V, Chacartegui R. Conceptualizing novel CH3OH-based thermochemical energy storage routes via a modeling approach. Cell Rep Phys Sci 2023;0:101357. https://doi.org/10.1016/J. XCRP.2023.101357.

[51] Chacartegui R, Sánchez D, Muñoz De Escalona JM, Jiménez-Espadafor F, Muñoz A, Sánchez T. SPHERA project: assessing the use of syngas fuels in gas turbines and combined cycles from a global perspective. Fuel Process Technol 2012;103: 134–45. https://doi.org/10.1016/J.FUPROC.2011.11.004.

[52] Carpenter SM, Long HA. Integration of carbon capture in IGCC systems. Integrat Gasific Combin Cycle (IGCC) Technol 2017;445–63. https://doi.org/10.1016/B978-0-08-100167-7.00036-6.

[53] Abagnale C, Cameretti MC, De Robbio R, Tuccillo R. CFD study of a MGT combustor supplied with syngas. Energy Procedia 2016;101:933–40. https://doi.org/10.1016/J.EGYPRO.2016.11.118.

[54] Ning D, Fan A, Yao H. Effects of fuel composition and strain rate on NO emission of premixed counterflow H2/CO/air flames. Int J Hydrogen Energy 2017;42: 10466–74. https://doi.org/10.1016/J.IJHYDENE.2016.12.059.

[55] Natarajan J, Lieuwen T, Seitzman J. Laminar flame speeds of H2/CO mixtures: effect of CO2 dilution, preheat temperature, and pressure. Combust Flame 2007; 151:104–19. https://doi.org/10.1016/J.COMBUSTFLAME.2007.05.003.

[56] Cuoci A, Frassoldati A, Buzzi Ferraris G, Faravelli T, Ranzi E. The ignition, combustion and flame structure of carbon monoxide/hydrogen mixtures. Note 2: fluid dynamics and kinetic aspects of syngas combustion. Int J Hydrogen Energy 2007;32:3486–500. https://doi.org/10.1016/J.IJHYDENE.2007.02.026.

[57] Zeng Q, Zhao M, Yuan Y. Hydrogen-rich fuel combustion characteristics of a counter dual-swirl combustor at fixed power. Energy Rep 2022;8:91–100. https://doi.org/10.1016/J.EGYR.2021.11.043.

[58] Ajvad M, Shih HY. Modeling syngas combustion performance of a can combustor with rotating casing for an innovative micro gas turbine. Int J Hydrogen Energy 2020;45:31188–201. https://doi.org/10.1016/J.IJHYDENE.2020.08.113.

[59] Pramanik S, Ravikrishna RV. Non premixed operation strategies for a low emission syngas fuelled reverse flow combustor. Energy 2022;254:124332. https://doi.org/10.1016/J.ENERGY.2022.124332.

[60] Chacartegui R, Torres M, Sánchez D, Jiménez F, Muñoz A, Sánchez T. Analysis of main gaseous emissions of heavy duty gas turbines burning several syngas fuels. Fuel Process Technol 2011;92:213–20. https://doi.org/10.1016/J. FUPROC.2010.03.014.

[61] Giles DE, Som S, Aggarwal SK. NOx emission characteristics of counterflow syngas diffusion flames with airstream dilution. Fuel 2006;85:1729–42. https://doi.org/10.1016/J.FUEL.2006.01.027.

[62] Thermoflow. THERMOFLEX. https://www.thermoflow.com (accessed September 16, 2023).

[63] Wu J, Brown P, Diakunchak I, Gulati A, Lenze M, Koestlin B. Advanced gas turbine combustion system development for high hydrogen fuels. Proc ASME Turbo Expo 2009;2:1085–91. https://doi.org/10.1115/GT2007-28337.

[64] IRENA and Methanol Institute. Innovation Outlook : Renewable Methanol. Abu Dhabi. 2021.

[65] Carlson M, BM-E. Techno-economic comparison of solar-driven SCO2 Brayton cycles using component cost models baselined with vendor data and estimates. ASME Digital Collection ASME Org; 2017.

[66] Carlson M, Middleton B, Ho C. Techno-Economic Comparison of Solar-Driven SCO2 Brayton Cycles Using Component Cost Models Baselined With Vendor Data and Estimates. 2017. https://doi.org/10.1115/ES2017-3590. p. V001T05A009.

[67] Michalski S, Hanak D, Production VM-J of C. Techno-economic feasibility assessment of calcium looping combustion using commercial technology appraisal tools. Elsevier; 2019.

[68] Michalski S, Hanak DP, Manovic V. Techno-economic feasibility assessment of calcium looping combustion using commercial technology appraisal tools. J Clean Prod 2019;219:540–51. https://doi.org/10.1016/J.JCLEPRO.2019.02.049.

[69] Michalski S, Hanak DP, Manovic V. Techno-economic feasibility assessment of calcium looping combustion using commercial technology appraisal tools. J Clean Prod 2019;219:540–51. https://doi.org/10.1016/J.JCLEPRO.2019.02.049.

[70] Bayon A, Bader R, Jafarian M, Energy LF-H. Techno-economic assessment of solid–gas thermochemical energy storage systems for solar thermal power applications. Elsevier; 2018.

[71] International Energy Agency I. Renewables 2022. 2022.

[72] Ho CK. A review of high-temperature particle receivers for concentrating solar power. Appl Therm Eng 2016;109:958–69. https://doi.org/10.1016/J. APPLTHERMALENG.2016.04.103.

[73] Tesio U, Guelpa E, Verda V. Integration of thermochemical energy storage in concentrated solar power. Part 1: Energy and economic analysis/optimisation. Energy Convers Managem X 2020;6:100039. https://doi.org/10.1016/J. ECMX.2020.100039.

[74] Steilen M, Jörissen L. Hydrogen conversion into electricity and thermal energy by fuel cells: use of H2-systems and batteries. Electrochem Energy Storage Renew Sources Grid Balanc 2015:143–58. https://doi.org/10.1016/B978-0-444-62616-5.00010-3.

[75] Götz M, Lefebvre J, Mörs F, McDaniel Koch A, Graf F, Bajohr S, et al. Renewable power-to-gas: a technological and economic review. Renew Energy 2016;85: 1371–90. https://doi.org/10.1016/J.RENENE.2015.07.066.

[76] Fasihi M, Weiss R, Savolainen J, Breyer C. Global potential of green ammonia based on hybrid PV-wind power plants. Appl Energy 2021;294:116170. https://doi.org/10.1016/J.APENERGY.2020.116170.

[77] Melin K, Nieminen H, Klüh D, Laari A, Koiranen T, Gaderer M. Techno-economic evaluation of novel hybrid biomass and electricity-based ethanol fuel production. Front Energy Res 2022;10:70. https://doi.org/10.3389/FENRG.2022.796104/BIBTEX.

[78] Badouard T, Moreira De Oliveira D, Yearwood J, Torres P. Final Report-Cost of Energy (LCOE) Study on energy costs, taxes and the impact of government interventions on investments in the energy sector. 2020.

[79] ETN Global. Hydrogen Deployment in Centralised Power Generation a Techno-economic CASE study Hydrogen Deployment in Centralised Power Generation-A Techno-Economic Case Study. 2022.

[80] Muñoz De Escalona JM, Sánchez D, Chacartegui R, Sánchez T. Part-load analysis of gas turbine & ORC combined cycles. Appl Therm Eng 2012;36:63–72. https://doi.org/10.1016/J.APPLTHERMALENG.2011.11.068.

[81] Chacartegui R, Sánchez D, Muñoz A, Sánchez T. Real time simulation of medium size gas turbines. Energ Conver Manage 2011;52:713–24. https://doi.org/10.1016/J.ENCONMAN.2010.07.050.

[83] Rozovskii AY, Lin GI. Fundamentals of methanol synthesis and decomposition. Top Catal 2003;22:137–50. https://doi.org/10.1023/A:1023555415577/METRICS.